

The effect of boundary conditions and ribs on the total radiation efficiency of submerged plates

Xia Pan, Ian MacGillivray and James Forrest

Maritime Division, Defence Science and Technology Group, Victoria, Australia

ABSTRACT

The radiation efficiency of a plate submerged in water is often used as a basis on which to represent the sound radiation from more complex underwater structures. The boundary conditions and stiffening ribs are known to have a significant influence on sound radiation from a plate for frequencies below the critical frequency. A numerical and analytical investigation of the radiation efficiency of submerged plates is presented in this paper. The total radiation efficiency is developed from a numerical finite element model using ANSYS by averaging the efficiency due to three point force positions. The effect of boundary conditions and ribs on the total radiation efficiency is discussed in detail. The basic results are compared with those from a numerical boundary element model using SYSNOISE and an analytical engineering formula. Excellent agreement is obtained between the two numerical methods. The analytical results agree well with the numerical ones over the whole frequency range except for some small regions.

1. INTRODUCTION

In naval applications, it is important to be able to estimate the noise radiated by a vibrating structure during its design stage. The radiation efficiency of a flat rectangular plate is often used as a benchmark to demonstrate the sound radiation from more complex plate-like structures. As it is difficult to measure the efficiency in water, most published experimental results have been for a plate in air, usually with an infinite (i.e. large) rigid baffle.

Initially, an analytical method was developed empirically by Maidanik (1962). He proposed approximate formulae for the efficiency in different frequency ranges of a simply supported plate in an acoustic baffle in air. Leppington *et al.* (1982) provided a detailed mathematical analysis of the radiation from modes of a simply supported panel including the multi-modal case. Their results mostly agreed with the formulae of Maidanik (1962) but they found a modified result close to the critical frequency. Oppenheimer and Dubowsky (1997) developed Maidanik's method to calculate an approximate efficiency of a plate without a baffle for frequencies below the plate critical frequency. They presented a corrected efficiency. The corrected efficiency contains scaling factors whose values were chosen empirically by comparison with measured data. Recently, Putra and Thompson (2010) extended Maidanik's method on a baffled plate in air to that on an unbaffled plate in air. They showed the difference in the efficiency between the baffled and unbaffled plates. Cheng *et al.* (2012) developed Maidanik's method for a baffled plate in water.

The boundary conditions and stiffening ribs have a significant influence on sound radiation from a vibrating structure for frequencies below its critical frequency. The critical frequency is where the structural wavenumber matches the acoustic wavenumber, and above which the whole plate surface contributes to very efficient sound radiation. Putra *et al.* (2014) presented an analytical model of the efficiency for a baffled plate in air using a discrete elementary source model. Variability of the efficiency for different forcing locations, and its average value, were discussed for several combinations of boundary conditions. Some experimental results were used to validate the analytical results.

However, previous work has not included detailed discussions of the efficiency of an unbaffled plate submerged in water, and has not compared with the efficiency of other numerical results. The sound radiation of an unbaffled plate submerged in water is a fundamental issue in maritime applications. The aim of the current work described here is to evaluate some numerical software capabilities to estimate the far field noise radiation from a vibrating underwater structure. Two numerical finite element / boundary element models are developed to evaluate the efficiency from a submerged unbaffled vibrating plate. An approximate analytical model is also presented. The effect of boundary conditions and ribs on the total efficiency of the plate is discussed using the numerical models. Some results from the numerical methods are compared with those from the analytical method.

2. THEORETICAL METHOD

2.1 Radiation Efficiency of a Baffled Plate in Air

The relation of radiation efficiency and radiated sound power given by Oppenheimer and Dubowsky (1997) is

$$\sigma = \frac{W_r}{\rho c S \langle \bar{V}^2 \rangle} \quad (1)$$

where W_r is the radiated sound power from one side of the plate if baffled or both sides of the plate if unbaffled, ρ is the density of the fluid, c is the speed of sound, S is the plate surface area and $\langle \bar{V}^2 \rangle$ is the spatially averaged mean-square normal velocity of the plate.

The total radiation efficiency for frequencies below the plate critical frequency has been presented by averaging radiation efficiencies of the modes of a simply supported baffled plate (Maidanik, 1962). The total efficiency of the simply supported baffled plate in air was expressed by Oppenheimer and Dubowsky (1997) as

$$\sigma_{baf} = \sigma_{comer} + \sigma_{edge}, \quad f < f_c \quad (2)$$

where σ_{comer} and σ_{edge} are the modal average radiation efficiencies for the corner and edge modes, and f_c is the critical frequency of the plate, which can be estimated by (Bies and Hansen, 1997)

$$f_c = \frac{0.55c^2}{c_L h} = \frac{0.55c^2}{h \sqrt{E/\rho_s(1-\nu^2)}}, \quad (3)$$

where h is the thickness of the plate, and c_L is the speed of longitudinal waves in the plate which can be expressed as shown in terms of the Young's modulus E , material density ρ_s and Poisson's ratio ν of the plate.

The terms corner and edge modes refer to the way that sound radiates from particular mode shapes below the critical frequency. In the interior of the plate, positive fluid displacement is balanced by neighbouring negative fluid displacement by a localised "fluid pumping" mechanism, with almost no resultant sound radiation. Depending on the mode, the only unbalanced fluid motion occurs at plate corners or plate edges, and hence sound radiation below the critical frequency can only occur from these regions. Above the critical frequency, sound radiates efficiently from the whole plate surface when the plate vibrates. Below the critical frequency, the radiation efficiency is less than unity and increases with frequency until it is about unity at and above the critical frequency. Dominant radiating regions (shaded) of a plate below the critical frequency are shown in Figure 1.

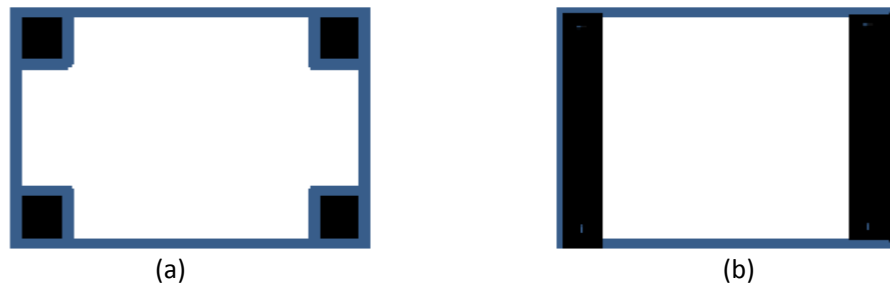


Figure 1: Dominant radiating regions (shaded) of a plate below the critical frequency:

(a) corner and (b) edge radiation.

For a baffled plate in air, Maidanik (1962) presented an approximation for σ_{comer} and σ_{edge} as follows

$$\sigma_{comer} = \frac{8}{\pi^4} \frac{\lambda_c^2}{S} \times \begin{cases} \frac{(1-2\alpha^2)}{\alpha(1-\alpha^2)^{1/2}}, & \alpha^2 < 0.5, \\ 0, & \alpha^2 \geq 0.5, \end{cases} \quad (4)$$

and

$$\sigma_{edge} = \frac{1}{4\pi^2} \frac{P\lambda_c}{S} \times \frac{\left\{ (1-\alpha^2) \log_e [(1+\alpha)/(1-\alpha)] + 2\alpha \right\}}{(1-\alpha^2)^{3/2}}, \quad (5)$$

where S is the plate area, P is the plate perimeter length, λ_c is the acoustic wavelength at the plate critical frequency and $\alpha = (f / f_c)^{1/2}$.

2.2 Radiation Efficiency of an Unbaffled Plate in Air

Oppenheimer and Dubowsky (1997) considered local hydrodynamic flows around a plate without an acoustic baffle to determine correction factors to apply to the radiation efficiency for a baffled plate. They presented the radiation efficiency for an unbaffled plate as

$$\sigma_{unb} = F_{plate}(F_{corner}\sigma_{corner} + F_{edge}\sigma_{edge}), \quad f < f_c. \tag{6}$$

F_{plate} is a plate correction that accounts for inertial flow interaction between both sides of the plate, with the greatest effect at low frequencies. F_{corner} and F_{edge} are local corrections which account for sound radiation from the corners and edges at higher frequencies. These corrections are shown below.

$$F_{plate} = \frac{\beta^4 k^4 S^2}{48\pi^2 \left(1 + \frac{\beta^4 k^4 S^2}{48\pi^2}\right)}, \tag{7}$$

where k is the acoustic wavenumber and β is the proportionality factor of the plate, which can be chosen by comparison with experimental or numerical data as will be shown below. Note that values of β can vary significantly with medium type and plate size.

$$F_{corner} = 0.5 \frac{13f}{f_c \left(1 + 13 \frac{f}{f_c}\right)} \tag{8}$$

and

$$F_{edge} = 0.5 \frac{49f}{f_c \left(1 + 49 \frac{f}{f_c}\right)}. \tag{9}$$

2.3 Radiation Efficiency of an Unbaffled Plate in Water

As an analytical method for an unbaffled plate submerged in water may not exist in literature, an approximate analytical method is presented in the current paper. The radiation efficiency from the analytical method was based on Equations (1) to (9). For a submerged plate in water, the density and sound speed of water were used. A single proportionality factor β in Equation (7) was chosen by comparison with numerical data and will be described in the following section.

3. NUMERICAL METHODS

Two numerical models were developed for predicting the radiation efficiency of an unbaffled plate in air or water. The first method is based on the finite element method (FEM) using the commercial software ANSYS. The second is the boundary element method (BEM) using the software SYSNOISE. A harmonic point force with amplitude of 1 N perpendicular to the plate was applied to calculate the velocity distribution and sound power. The total radiation efficiency was calculated by averaging the efficiencies due to three point force positions as shown in Figure 2.

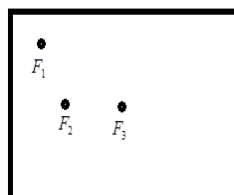


Figure 2: Positions of point forces used in the numerical methods.

3.1 ANSYS Method

For the finite element model, ANSYS Acoustics was used and the damping loss factor 0.02 was included. Figure 3 shows the ANSYS model used to calculate sound radiation. In order to calculate the radiation of submerged structures in water, a fully coupled structural acoustic model was developed. The fully coupled model consisted of the plate structure and two acoustic bodies. One acoustic body was a computational domain enclosing the plate with fluid. The other was a perfectly matched layer (PML) enclosing the computational domain with fluid to simulate the infinite boundary of sea water. The sizes of the acoustic bodies were determined by considering the longest acoustic wavelength, and the element size was determined by the shortest wavelength. Specifically, the element size was chosen to ensure at least six elements per wavelength. The size of the computational domain was at least half of the wavelength, and the size of the PML was at least one quarter of the wavelength, as recommended by ANSYS Acoustics guidelines. The meshes of the plate and two acoustic bodies were connected. The fully coupled analysis accounts for the fluid-structure interaction.

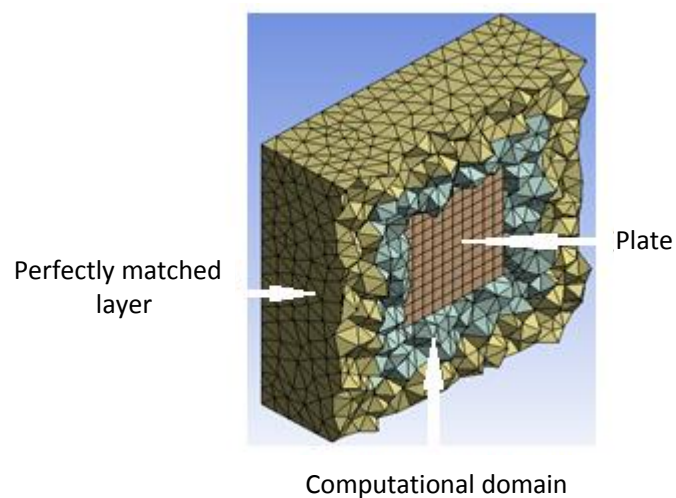


Figure 3: FE (ANSYS) model showing a plate, computational domain and perfectly matched layer of the section plane.

3.2 SYSNOISE Method

Using SYSNOISE for the BEM, the plate was modelled as structural two-dimensional shell finite elements while the acoustic domain was modelled using the indirect boundary element method (BEM). The BEM did not include intrinsic plate damping. The indirect BEM allows fluid to exist on both sides of the plate, thereby representing an un baffled plate. The coupling in this case was specified using the SYSNOISE fluid-structure link.

In this problem, SYSNOISE does not calculate the radiation directly from the forced plate, but uses a modal basis approach. Specifically, SYSNOISE is initially used to compute the in-vacuum modes of the plate and then the plate is coupled to the fluid medium in order to compute the coupled modes. These modes are computed to well above the upper frequency of the required radiation efficiency. The forced response is then obtained in terms of these coupled modes. The total radiated power, plate vibration (as mean-square velocity), and radiation efficiency are all obtainable directly from the SYSNOISE calculation.

4. RESULTS

The numerical and analytical results to be presented here have been calculated for steel square plates with side length 0.2 m and thickness 0.003 m. The critical frequency for all submerged plates is $f_c = 78\text{kHz}$, while for the plates in air it is $f_c = 4\text{kHz}$. All the results shown below are for un baffled plates which have either four clamped edges or combinations of clamped and free edges. For the ANSYS modelling, 1600 elements for the plate, 38053 elements for the computational domain and 53317 elements for the PML were required. For the SYSNOISE modelling, over 500 modes up to 100 kHz, and a mesh resolution of 2.5 mm, giving 6400 plate elements, were

required to compute consistent values of radiation efficiency up to the critical frequency of the plate. The fluid region is not meshed for the BEM calculation.

4.1 Numerical Results

Numerical results for the radiation efficiency are initially presented for a plate with a central normal force excitation (see F_3 in Figure 2). The total efficiency is obtained by averaging results for the three force positions and will be shown in next section.

4.1.1 Effect of Water Loading

Figures 4(a) to (c) show the first three modal shapes and natural frequencies of a clamped plate in air using the ANSYS method. Figures 4(d) to (f) show the results for the plate in water. The results shown in Figure 4 indicate the effect of water loading reduces the natural frequencies by mass loading. The mode shapes remain the same for modes 1 and 3, while the shape of mode 2 in Figure 4(e) is likely a linear combination of the two possible mode shapes at the same frequency because of the plate symmetry (one with the vertical nodal line as in Figure 4(b), and one with a horizontal nodal line).

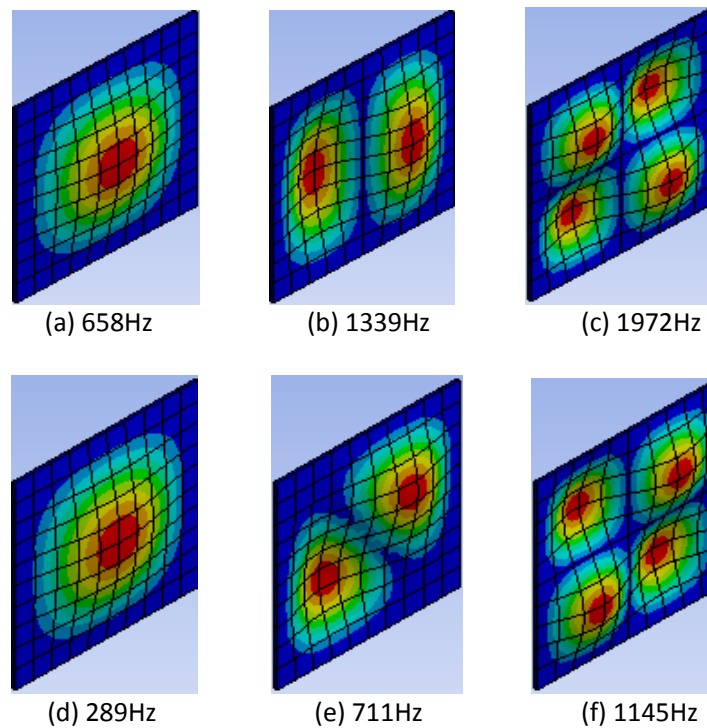


Figure 4: First three modal shapes and natural frequencies of a clamped plate using FEM: (a)-(c) plate in air; (d)-(f) plate in water.

Figure 5(a) shows the comparison of the radiation efficiencies obtained from the ANSYS and the SYSNOISE methods for the plate in air. Figure 5(b) shows the results for the plate in water. Results shown in Figure 5 indicate that the effect of water loading is a reduction in the efficiency for the same frequency range, which is due to the increased wavelength in water. In other words, the 2 kHz range shown is a much smaller fraction of the critical frequency for the plate in water than in air; the equivalent fraction for the plate in air implies the frequency range to about 100 Hz, where the efficiency is similarly very low. Excellent agreement is obtained between the two methods.

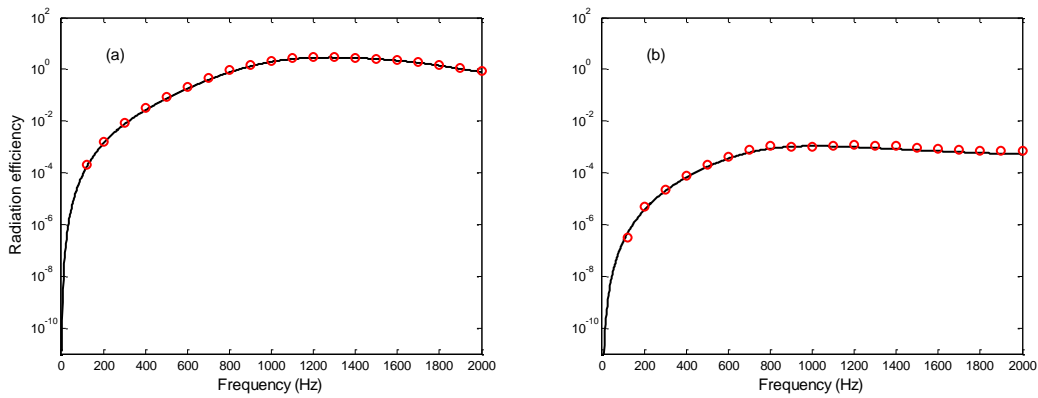


Figure 5: Radiation efficiency of the clamped plate: (a) in air; (b) in water. —, from BEM; ○ ○ ○, from FEM.

4.1.2 Effect of Boundary Conditions

In this case, submerged plates with three different boundary conditions are considered. They are either plates with all edges clamped or two combinations of clamped and free edges. The natural frequencies of the clamped plate (CCCC) have been given in Figures 4(d) to (f). Figures 6(a) to (c) present the first three modal shapes and natural frequencies of a plate with three edges clamped and one edge free (CCCF) by using the ANSYS method. Figures 6(d) to (f) present the results for a plate with two edges clamped and two edges free (CCFF). Comparing Figures 4(d)-(f) with Figure 6 shows that increasing the boundary constraint generally increases the natural frequencies by increasing the structure’s overall stiffness.

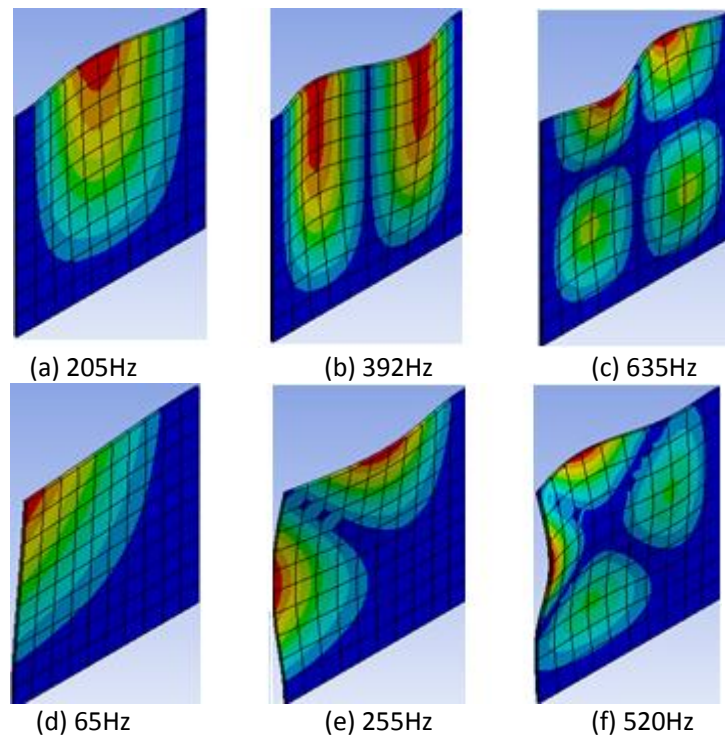


Figure 6: First three modal shapes and natural frequencies of a submerged plate using FEM: (a)-(c) CCCF plate with top edge free; (d)-(f) CCFF plate with top and left edges free.

Figure 7 shows comparisons of the efficiencies calculated from the ANSYS and SYSNOISE methods. Figure 7(a) shows the radiation efficiency of a CCCF plate and Figure 7(b) shows the result for a CCFF plate. The dips in the efficiencies presented in Figure 7 are caused by dips in the radiated power. Phasing of the different parts of the plate vibration is such that sound radiation is cancelled at the frequencies where the dips occur. Results shown in Figure 7 demonstrate good agreement between the two methods for the CCCF and CCFF plates.

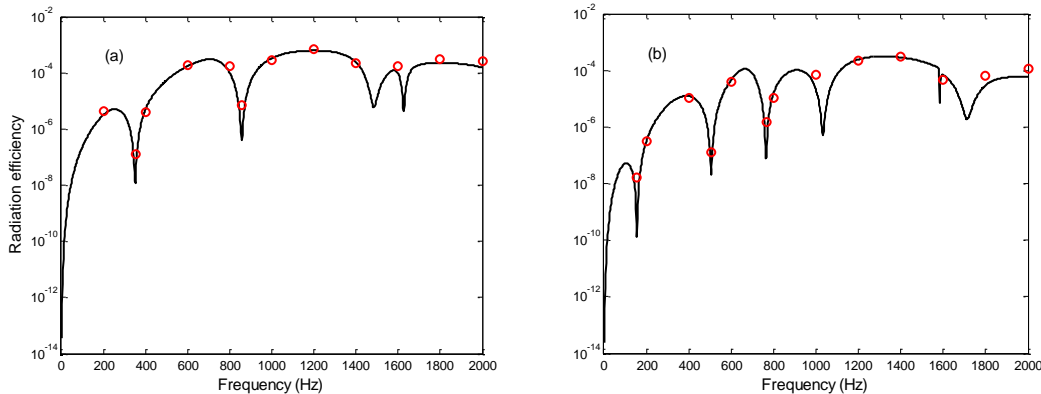


Figure 7: Radiation efficiency of the submerged plate. (a) CCCF plate; (b) CCFF plate. —, from BEM; ○ ○ ○, from FEM.

To demonstrate the effect of boundary conditions on the radiation efficiency, Figure 8 shows the comparison of the efficiencies of the CCCC, CCCF and CCFF plates using the SYSNOISE method. It can be seen that increasing boundary constraint generally gives an increase in the efficiency. This is possibly because the reduction in the degrees of freedom of the plate makes the plate motion more uniform (and therefore more like that of an oscillating piston), which has a higher radiation efficiency. Note that increased efficiency does not necessarily mean higher absolute radiated sound power for a given structural force, as the mean-square velocity of a more constrained plate could be lower for that force than the mean-square velocity of a more free plate.

Note that the radiation efficiency below the critical frequency depends on how the plate is excited as well. The effect of excitation type is beyond the scope of the current paper.

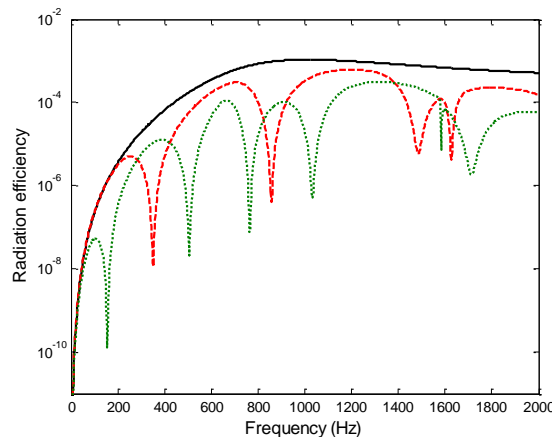


Figure 8: Radiation efficiency of the submerged plate using BEM. —, CCCC plate; - - -, CCCF plate; • • •, CCFF plate.

4.1.3 Effect of Ribs

In this section and the following section, the modelling frequency range is extended up to 75000 Hz in order to view the efficiency just below the critical frequency ($f_c = 78\text{kHz}$).

To demonstrate the effect of ribs on the efficiency of a plate, a rib with width 20mm and thickness 6 mm was placed across the centre line of one side of the clamped plate (CCCC). Figures 9(a) to (c) show the first three modal shapes and natural frequencies of the clamped ribbed plate in air using the ANSYS method. Figures 9(d) to (f) show

the results for the plate in water. The effect of water loading decreases the natural frequencies of the ribbed plate, as before. Comparing the results shown in Figure 4 without a rib, it is found that the ribbing increases the natural frequencies by increasing the stiffness of the plate.

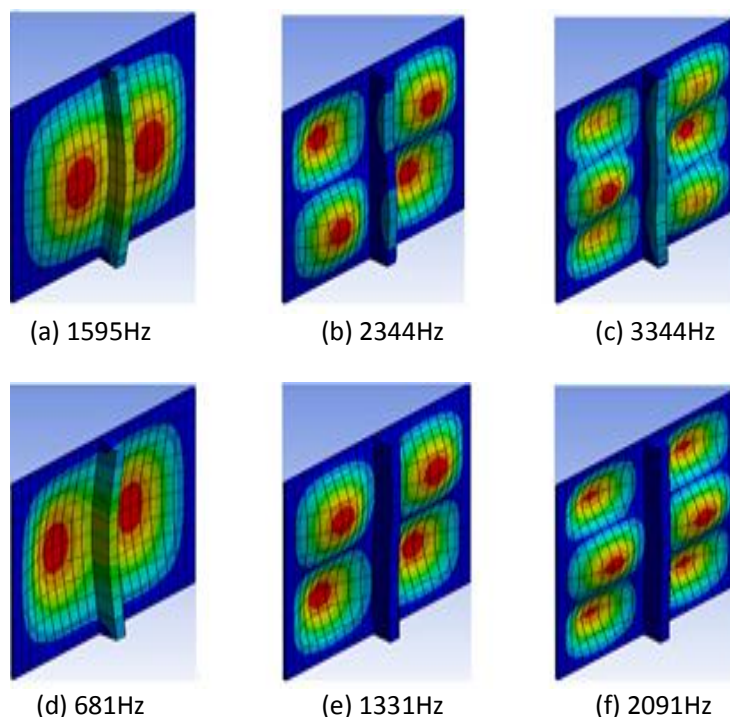


Figure 9: First three modal shapes and natural frequencies of a clamped ribbed plate using FEM: (a)-(c) plate in air; (d)-(f) plate in water.

Figure 10 shows the comparison of the efficiencies of a submerged clamped plate with and without a rib using the ANSYS method. The analysis shown in Figure 10 predicts that the ribbing slightly increases the efficiency, especially for frequencies above 1 kHz. It is expected that more ribs will further increase the efficiency. This is because stiff ribs effectively add more constrained edges to the plate, which can generate sound radiation below the critical frequency in the same way that the outside edges of the plate can generate sound radiation.

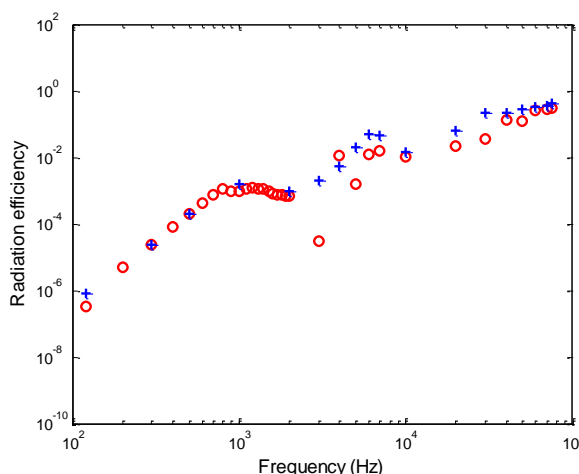


Figure 10: Radiation efficiency of the submerged clamped plate with and without a rib from FEM.
 ○ ○ ○, without the rib; + + +, with the rib.

4.2 Comparison with Analytical Results

The total efficiency obtained from the analytical method by averaging the efficiencies of modes (see Section 2.1) was used to validate the numerical methods. For a submerged plate in water, the proportionality factor $\beta = 8$ in Equation (7) was chosen empirically by comparison with the numerical data. For an initial comparison, the efficiencies obtained from the two numerical methods due to one central force excitation are used as a benchmark to compare with the total efficiency obtained from the analytical method.

Figure 11 shows the comparison of the efficiencies of the submerged clamped plate without a rib from the analytical and the two numerical methods. Agreement is obtained between the two numerical methods. The analytical result agrees less well with the numerical ones at frequencies between 1200Hz and 3700Hz, especially the dip at 3000 Hz. This is because the analytical result is obtained as the average over all modes, while the numerical results are for one central force excitation, which will not excite the modes with central nodal lines.

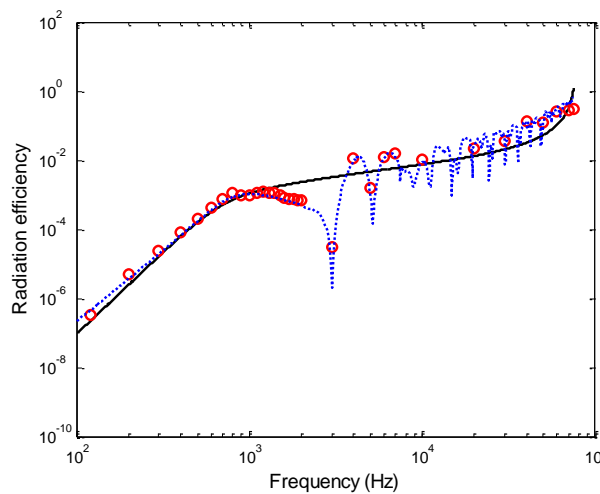


Figure 11: Radiation efficiency of the submerged clamped plate. —, from the analytical method (total efficiency); ○ ○ ○, from FEM; • • •, from BEM.

The total efficiencies from both numerical methods were obtained by averaging three force positions (see Figure 2). Figure 12 presents the comparison of the total efficiencies obtained from the analytical and the two numerical methods. It can be seen that the dip at 3000 Hz is reduced due to the averaging.

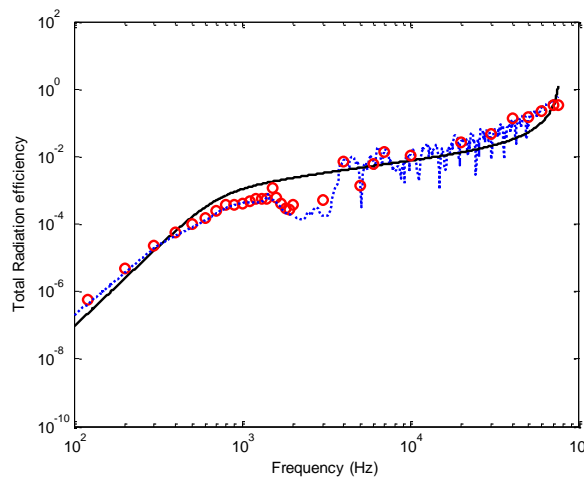


Figure 12: The total radiation efficiency of the submerged clamped plate. —, from the analytical method; ○ ○ ○, from FEM; • • •, from BEM.

5. CONCLUSIONS

Two numerical finite element / boundary element models have been developed for predicting the total radiation efficiency of an unbaffled plate below the critical frequency when submerged in water. As an analytical model for an unbaffled plate submerged in water may not exist in the literature, an approximate analytical model has been presented. The analytical model contains a single scaling factor which is chosen by comparison with experimental or numerical data.

The effect of water loading on the plate was evaluated using the two numerical methods. As expected, it was found that water loading reduced plate natural frequencies by mass loading. The efficiency for the same frequency range was also reduced due to the increase in acoustic wavelength and consequently much higher critical frequency for the plate in water.

The effects of various boundary conditions and rib inclusion on the total efficiency were investigated using the numerical methods. It was found that increasing the boundary constraint or including ribs on the plate had similar effects in terms of the natural frequencies and the efficiency below the critical frequency. Specifically, the boundary constraint or ribs generally increased the natural frequencies, and gave an increase in the efficiency due to constrained boundaries increasing the overall stiffness of the plate or due to the ribs increasing the effective constrained edge length.

Excellent agreement has been obtained between the two numerical methods. The analytical method agrees well with the numerical solutions over the whole frequency range except for some small regions. This is believed to be due to inadequate averaging with the numerical methods.

6. REFERENCES

Bies, D.A. and Hansen, C.H. 1997, *Engineering Noise Control: Theory and Practice*, 2nd edition, London: Spon Press.

Maidanik, G. 1962, 'Response of ribbed panels to reverberant acoustic fields', *Journal of the Acoustical Society of America*, **34**, pp. 809-826.

Leppington, F.G., Broadbent, E.G., and Heron, K.H. 1982, 'The acoustic radiation efficiency of rectangular panels', *Proceedings Royal Society, London, Series A* 382, 245-27.

Oppenheimer, C.H. and Dubowsky, S. 1997, 'A radiation efficiency for unbaffled plates with experimental validation', *Journal of Sound and Vibration*, **199**, pp. 473-489.

Putra, A. and Thompson, D.J. 2010, 'Sound radiation from rectangular baffled and unbaffled plates', *Applied Acoustics*, **71**, pp. 1113-1125.

Cheng, Z., Fan, J., Wang, B. and Tang, W. 2012, 'Radiation efficiency of submerged rectangular plates', *Applied Acoustics*, **73**, pp. 150-157.

Putra, A., Shyafina, N., Thompson, D.J., Muhammad, N., Jailani, M., Nor, M. and Nuawi, Z. 2014, 'Modelling sound radiation from a baffled vibrating plate for different boundary conditions using an elementary source technique', *Proceedings Inter-Noise 2014, Melbourne, Australia*.

7. ACKNOWLEDGEMENTS

The authors would like to thank Dr. Li Chen for proposing this project.